Research Article

Characterization of raw and thermally treated Nigerian kaolinite-containing clays using instrumental techniques

Funmilayo I. Adeniyi[1,2] · Mary B. Ogundiran[1] · T. Hemalatha[2] · Bhajantri Bharatkumar Hanumantrai[2]

Received: 13 January 2020 / Accepted: 26 March 2020 / Published online: 5 April 2020

Abstract
Thermal behavior, surface area, oxide, mineralogical composition, and structural functional groups of raw and thermally treated five local kaolin clays [Ijero-Ekiti (IJ), Ikere-Ekiti (IK), Isan-Ekiti (IS), Abusoro (AB) and Odigbo (OD)] from two states in South-West Nigeria were studied in order to determine their potential uses. These properties were measured using thermogravimetric analysis coupled with differential thermal analysis (TGA/DTA), surface area and porosity analysis, X-ray fluorescence (XRF), X-Ray Diffractometry (XRD) and Fourier Transform infra-red spectroscopy (FTIR) respectively. The TGA/DTA showed major mass losses and broad endothermic bands at temperatures 390–700 °C, which were associated with dehydroxylation of kaolinite and other clay minerals. Thermal treatment increased the surface area of the raw clays. The XRF results showed oxides of kaolinite, illite, quartz, feldspar, hematite, anatase and the phases were confirmed by XRD. The FTIR spectra displayed the characteristic absorption bands of the minerals. Combining the obtained results, Ijero-Ekiti clay was identified as feldspar (albite)-quartz containing clay, Ikere-Ekiti and Isan-Ekiti clays as kaolinite-dominated clays, Abusoro clay as kaolinite-illite-montmorillonite-containing clay and Odigbo clay as kaolinite-illite-containing clay. The TGA/DTA, XRD and FTIR indicated that crystalline kaolinite in the clays were converted into amorphous metakaolinite after thermal treatment. Based on the properties displayed, clays from IK, IS, AB and OD deposits can be thermally treated to form useful supplementary cementitious and geopolymer materials to make binders in building and construction while clay from IJ deposit can be a potential raw material for ceramic production.

Keywords Nigerian kaolinite clays · 2:1 clay minerals · TGA/DTA · XRF · XRD · FTIR

1 Introduction

Kaolinite-containing clay as a gift from nature has been applied for various uses due to its physicochemical characteristics. Kaolin clays contain kaolinite, one of the clay minerals, that has been widely used for various purposes due to its high content of silica and alumina. From the past, its uses include industrial applications in paints, ceramics, electrical insulators, cosmetics and rubber production among others [1–3]. Lately, the application of kaolinite (or in form of metakaolinite) for catalyst production, carbon sequestration, supplementary cementitious and geopolymer starting materials are receiving global attention. Kaolin clays both in the raw and thermally treated forms have been used to synthesize aluminosilicate materials for catalytic applications [4, 5]. It was also applied to produce kaolin-based cement plug as an alternative to OPC plugs for upstream carbon sequestration [6]. Its current use as supplementary cementitious materials is on the increase [7–13]. This is due to global demand for cement by construction and building industry. Supplementary cementitious materials are used to replace part of OPC so as to reduce energy requirement and enormous emission of CO_2 during cement manufacturing. The CO_2 is one of the

✉ Mary B. Ogundiran, mbogundiran@gmail.com | [1]Analytical/Environmental Unit, Department of Chemistry, University of Ibadan, Ibadan, Oyo State, Nigeria. [2]CSIR-Structural Engineering Research Center, Chennai, Tamilnadu, India.

leading causes of climate change, which results in global warming. To reduce this emission, local kaolin clays due to their availability and the reactive nature of their thermally treated forms, are being considered as supplementary cementitious materials to replace parts of cement. Thermal treatment of kaolin clays gives rise to formation of amorphous material which can produce reactive silicate and aluminate species. These species are capable of reacting with calcium hydroxide solution that forms during cement hydration to generate stable insoluble compounds (calcium-silicate-hydrate and calcium-aluminate-hydrate) which possesses cementitious properties [8, 12, 14, 15]. Apart from CO_2 emission reduction, other advantages of substituting some portion of cement with metakaolin have been documented to include lower heat of hydration, higher density, improved strength and resistance to degradation mechanisms [11].

Pure metakaolin or thermally treated local kaolin clay is one of the main materials used for production of geopolymers. Geopolymer is an inorganic aluminosilicate material that similarly functions as a binder used for various purposes. It is also undergoing consideration as an alternative to ordinary Portland cement. Authors have reported the use of pure metakaolin and locally available kaolin clays as suitable materials for producing geopolymers [16–20]. Kaolin clays are useful as geopolymer materials because they contain high silica and alumina species which react with alkaline silicate solution to form inorganic binders called geopolymer.

The alumina and silica in kaolin clays exist in crystalline unreactive states. This creates necessity for thermal treatment which transforms the kaolinite into amorphous reactive metakaolinite. This expands the scope of usefulness of kaolin clays. Thermal treatment of kaolinite at temperatures within 400–750 °C has been documented to result in its dehydroxylation to metakaolinite [21, 22]. Sometimes kaolinite is accompanied by other clay and associated minerals depending on its geological origin. These minerals give each kaolin clay its unique properties which also affect its reactivity [15] and functionality. The properties that affect functionality of kaolin clays include physical characteristics, chemical composition, mineralogical phases, structural functional groups and thermal behavior [23]. X-ray fluorescence (XRF) spectroscopy, X-Ray diffraction (XRD), Fourier transform infrared (FTIR) spectroscopy, thermogravimetric analysis (TGA) and differential thermal analysis (DTA) are usually used for the determination of the chemical composition, mineralogical phases, structural functional groups and structural changes upon thermal reaction.

Investigations are ongoing globally on the suitability of using locally available kaolinite-containing clays for various purposes [1, 3, 4, 7, 9, 16, 18]. Nigeria is blessed with deposits of kaolin clays, although with varied purity. However, the potentials of these kaolin clays have not been widely studied due to lack of scientific knowledge about their properties. In the past, kaolin clay has been used primarily in Nigeria for production of pottery, molding bricks and sculpture. Recently, researchers have been experimenting with Nigerian kaolin as ceramic materials, cement replacement [24, 25] and also as geopolymer materials [16]. Kaolin clays deposits are widely spread in Nigeria and if their properties are known, they can serve as good sources of ceramics, supplementary cementitious and geopolymer materials, and for other uses.

The focus of this study therefore, was to characterize both raw and thermally treated five Nigerian kaolinite-containing clays from different deposits in South West Nigeria using various characterization techniques. These clays have been underutilized due to lack of knowledge about their properties which are scarce in literature. The scientific understanding of the properties of these clays will enhance their applications. In order to investigate the chemical composition, thermal reactions, mineralogical phases, structural functional groups, the clays in their raw and thermally treated states were subjected to X-ray fluorescence (XRF) spectroscopy, thermogravimetric analysis coupled with differential thermal analysis (TGA/DTA), X-ray diffraction (XRD) and Fourier Transform infrared (FTIR) spectroscopy.

2 Materials and methods

2.1 Materials

Five natural kaolin clays were obtained from their deposits in two states in South-western Nigeria. The clays named Ijero-Ekiti (IJ), Ikere-Ekiti (IK) and Isan-Ekiti (IS) were collected from deposits in Ijero, Ikere and Oye Local Governments of Ekiti state, while Abusoro (AB) and Odigbo (OD) were collected from deposits in Okitipupa and Odigbo Local Governments in Ondo state. The clays were physically differentiated by their colors (Fig. 1). The clays were air-dried for 3 days, crushed and sieved to 212 µm with a standard sieve.

2.2 Sample characterisation

2.2.1 Simultaneous thermal analysis

Simultaneous thermal behaviors of the raw clays which included thermogravimetric analysis (mass loss changes) and differential thermal analysis (TGA/DTA) were measured with NETZSCH STA 449 F3 *Jupiter* thermal analyzer. The temperature range of the analyzer was set at 40–900 °C

Fig. 1 Colors of the raw clays

with a heating rate of 10 °C per minute under nitrogen atmosphere.

2.3 Production of thermally treated clays

The clays were thermally treated in a programmable furnace for 6 h according to Ogundiran and Kumar [16] at their various maximum dehydroxylation temperatures. The IJ and OD clays were heated at 650 °C, while AB, IK and IS clays were heated at 700 °C as shown by their respective DTA curves. The raw clays were designated as RIJ, RIK, RIS, ROD and RAB while the thermally treated clays were labelled as TIJ, TIK, TIS, TOD and TAB. These samples were analyzed with the selected characterization techniques as shown below.

2.4 Surface area (BET method) and porosity analysis

The surface area and pore size distribution of the raw and thermally treated clays were measured based on physical adsorption–desorption of N_2 gas on the surface of the clays using Surface Area and Porosity Analyzer (Micromeritics ASAP 2020-V4.03). The raw and thermally treated clays were degassed by oven drying at 105 °C for 6 h to remove moisture. Specific surface area was determined using Brunauer-Emmet-Teller (BET) method and volume of pores in the samples by Barrett-Joyner-Halenda (BJH) method.

2.5 X-ray fluorescence analysis of the clays

Oxide composition of the thermally treated clays was determined using Energy Dispersive X-Ray Fluorescence Spectrometer (EDX3600B) with a filament current of 350μA and an accelerating voltage of 40 kV.

2.6 X-ray diffraction analysis of the clays

The XRD patterns of mineral phases in the raw and mineral phase transformations in the thermally treated clays were obtained from D2 Phaser Bruker XRD difractometer using X-ray powder diffraction technique. The sample conditions were 2θ range from 5° to 80° with a scan speed of 0.02°/0.5 s. The CuKα radiation was generated with an accelerating voltage of 30 kV and filament current of 10 mA and the detector used was Lynxeye.

2.7 Fourier transform infra-red analysis of the clays

Structural functional groups of the raw and thermally treated clays were identified by FTIR spectrometer (FT/IR-4700typeA) set to scan frequencies across a range of 4000 to 400 cm^{-1} with a resolution of 4 cm^{-1}. Sample preparation was done by KBr pellet technique.

3 Results and discussion

3.1 Thermogravimetric and differential thermal analyses (TGA/DTA) of the clays

The results of thermogravimetric and differential thermal analysis of the clays (Fig. 2) showed that the weight loss and the temperature at which thermal reaction occurred differed for the different clays. The DTA curves for the clays were characterized with three mass losses and three endothermic peaks. The initial portion of TGA and DTA (temperatures of 100–200 °C) curves showed an insignificant weight loss of 0.04 (IK and IS), 0.06 (IJ), 0.12 (OD), 0.26 (AB) % during the first endothermic reaction which signified loss of adsorbed and interlayer water (nH_2O). The higher water loss demonstrated by OD and AB were possibly due to the presence of hydrated 2:1 clay mineral which contains interlayer water. Clays are differentiated by their chemical and mineralogical compositions as well as their structure. Clay mineral structure consists of silicon tetrahedrons (four-coordinated Si) and alumina octahedrons (six-coordinated Al) primarily. There are different clay group minerals depending on the ratio of silica to alumina (SiO_2/Al_2O_3) and how their sheets are layered. The 1:1 clay minerals consist of tetrahedral-octahedral sheet where silica and alumina sheets form a layer by shared oxygen atoms and the layers are held together by hydrogen bonding; kaolinite is an example in this group. On the other hand, the sheet may be layered in a 2:1 to form tetrahedral-octahedral-tetrahedral where silica, alumina and silica sheets form a layer by shared oxygen atoms with interlayer space where adsorbed water molecules and or ions are found. Montmorillonite, illite and chlorite are examples of clay minerals in this group [26, 27].

The oxide composition and XRD patterns of OD and AB confirmed that they contained 2:1 clay group {illite $(K,H_3O)(Al,Mg,Fe)_2(Si,Al)_4O_{10}(OH)_2,(H_2O)$, and montmorillonite $(Na,Ca)_{0.33}(Al,Mg)_2Si_4O_{10}(OH)_2{\cdot}n(H_2O)$}which are hydrated. A more rapid and major weight loss was observed at 390–650, 430–650, 440–700, 450–700 and 440–700 °C for IJ, OD, IS, IK and AB, respectively. This represents the beginning and completion of dehydroxylation of kaolinite in the clays. However, it has been documented that apart from kaolinite, other hydroxylated clay minerals also show endothermic reactions within these temperature ranges due to dehydroxylation of their octahedral sheet. Some

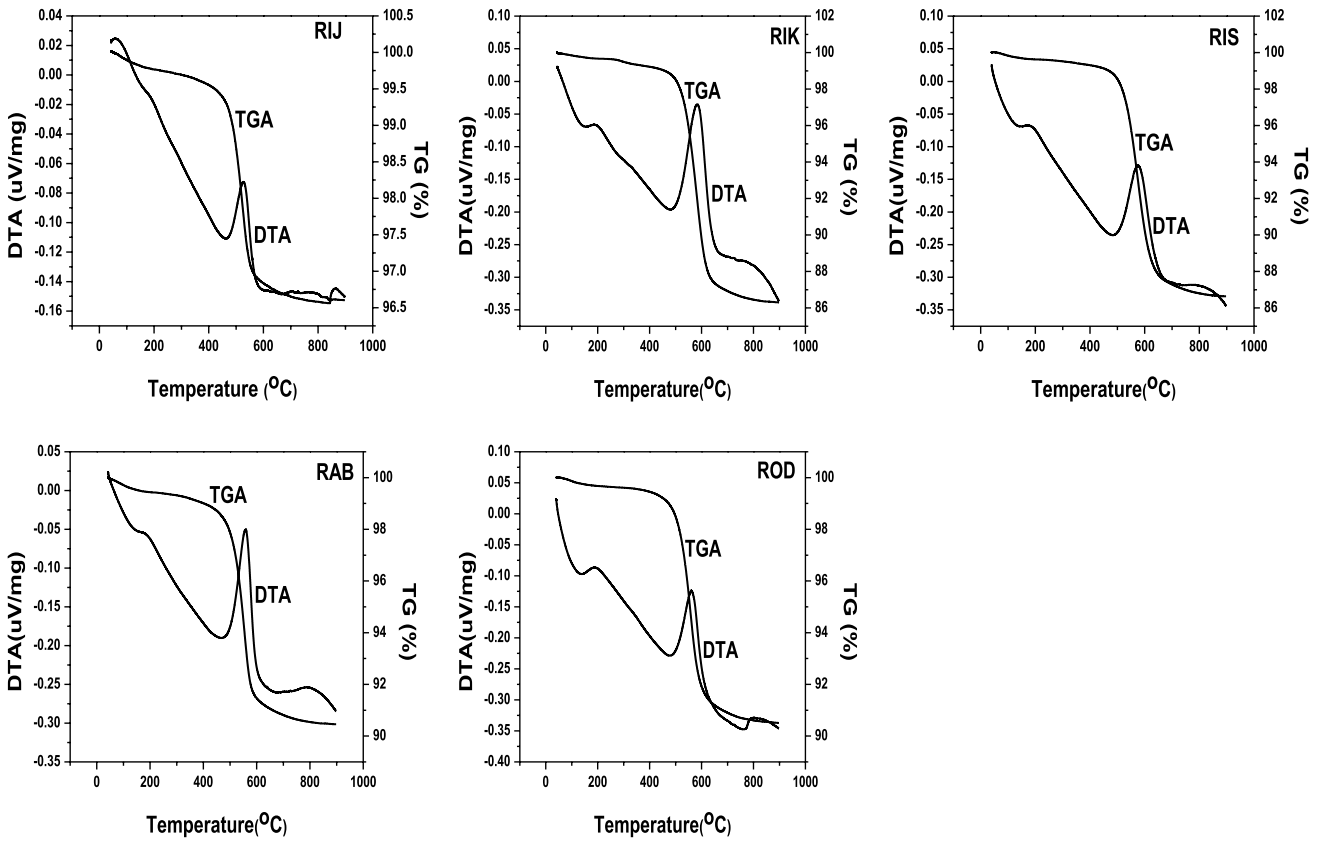

Fig. 2 TGA/DTA curves of raw clays

authors reported overlap of dehydroxylation of other aluminosilicate clay minerals like chlorite, illite and montmorillonite within these temperatures [12, 28–31]. The mass losses at these temperatures were 2.9%; 7.9%, 8.1%; 11.9%; 12.2%, for IJ, AB, OD, IS and IK clays, respectively. The high mass losses for the clays except IJ at the dehydroxylation temperature are indications that the clays contained highly reactive kaolinite. The extent of mass loss showed the degree of dehydroxylation for each clay and this was higher for IK and IS. This is also consistent with their XRD pattern, where IK and IS indicated the formation of large proportion of amorphous material (Fig. 7).

The endothermic reaction of IJ at 390–650 °C may be attributed to dehydroxylation of small amounts of kaolinite and other clay minerals contained in the clay overlapping with transition of α-quartz (SiO_2) to β-quartz (SiO_2). As already documented [32, 33], the endothermic reaction of quartz at around 573 °C corresponds to structural transition of trigonal (alpha) to hexagonal (beta). Based on this fact, if IJ contained only quartz, mass change was not expected to occur at these temperatures for IJ. However, a small mass change of about 2.9% occurred. This might be an indication of dehydroxylation of clay minerals. The presence of trace amounts of kaolinite and illite was later supported by XRD pattern and FTIR of IJ. The XRD pattern of IJ also revealed the presence of feldspar in the form of albite ($NaAlSi_3O_8$). Nevertheless, albite also remained stable to heat at this temperature [33]. Additional mass losses (0.03, 1.11, 1.22 and 2.12%) were observed at the third endothermic peaks between 700 and 900 °C for IJ, OD, AB, IS and IK. This third broad and low intensity endothermic peak has been associated with the presence of 2:1 clay minerals [12]. This temperature interval was documented as the temperature at which the final structural breakdown of 2:1 clay minerals (montmorillonite and illite) occurs [12, 18, 31, 34]. This is in agreement with the results of XRD analysis where Illite was detected in IK, IJ, IS and OD, while montmorillonite and illite were detected in AB (Fig. 6) at their maximum dehydroxylation temperatures.

3.2 Surface area and porosity analysis

The BET surface area of the raw clays were in the range of 2.30–16.2m^2/g, while that of thermally treated clays increased from 2.78 to 17.5m^2/g in Table 1. Raw Ijero clay (RIJ) and its thermally treated form had the lowest value compared to raw Abusoro clay and its thermally treated form. These results indicated that the BET surface areas increased with thermal treatment of the raw clays [35]. The t-plot micropore areas decreased from the raw clays to the thermally treated clays except for ROD and TOD in Table 1. Furthermore, the values of the micropore areas were smaller than the external surface areas except for RIJ and RIS, indicating that the external surface area was the major active surface for the clays [36].

According to International Union of Pure and Applied Chemistry (IUPAC), the adsorption–desorption isotherms of the raw and thermally treated clays correspond to Type IV isotherm in Fig. 3, these isotherms are illustrated by a limited uptake over a series of high relative pressure and a hysteresis loop [36–38]. The first part of the adsorption isotherms in the range of low relative pressures (0.02–0.7) was due to monolayer-multilayer adsorption, while the second section was associated to adsorption by capillary condensation in the mesopores [36, 37]. The hysteresis of the adsorption isotherms of the raw and thermally treated clays in Fig. 3 corresponds to H3 hysteresis pattern, which suggests that their pores are narrow and slit-shaped having average pore diameter of 118–213 Å for the raw clays and 125–187 Å for the thermally treated clays as shown in Table 1 [36].

The pore size distribution and the cumulative pore volume of the clays were analyzed using Barrett-Joyner-Halenda (BJH) model on the adsorption isotherms and

Table 1 BET surface area and pore sizes of raw and thermally treated clays

Source materials	BET surface area (m^2/g)	BJH desorption average diameter (Å)	t-plot External surface area (m^2/g)	t-plot Micropore area (m^2/g)
RIJ	2.30 (±0.08)	117.7	-0.77	3.07
ROD	5.69 (±0.01)	173.2	4.99	0.70
RIS	5.67 (±0.14)	246.6	0.79	4.88
RIK	7.63 (±0.03)	236.8	6.00	1.63
RAB	16.2 (±0.09)	213.4	12.2	4.00
TIJ	2.78 (±0.03)	125.2	1.86	0.92
TOD	6.30 (±0.02)	171.0	5.50	0.79
TIS	7.73 (±0.01)	187.1	7.09	0.64
TIK	8.92 (±0.04)	215.5	7.57	1.36
TAB	17.5 (±0.06)	187.4	15.2	2.29

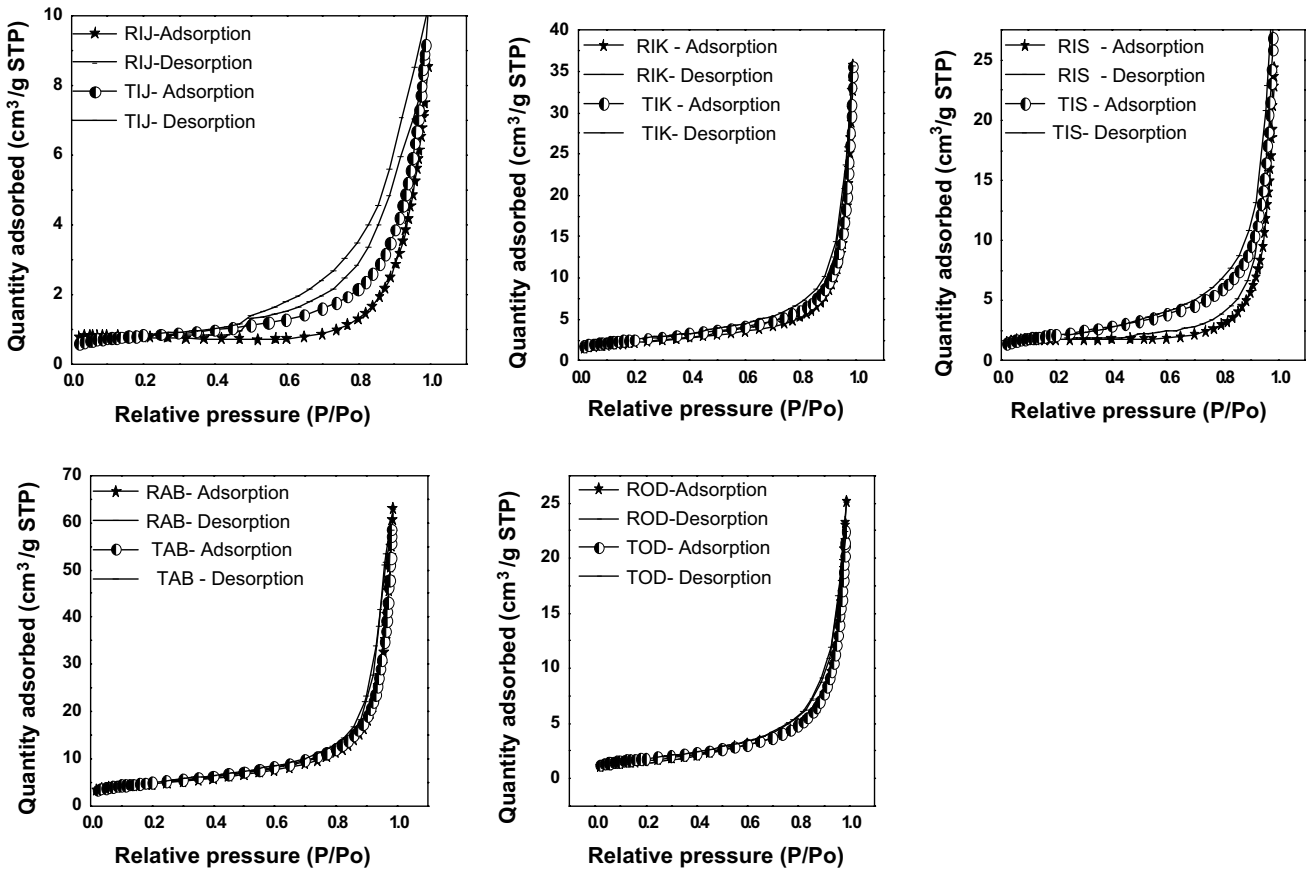

Fig. 3 Isotherm linear plot of raw and thermally treated clays

presented in Figs. 4 and 5. The volume of pores available for interaction with the N_2 gas increased from the raw to the thermally treated clays. The presence of mesopores was observed in the raw and thermally treated clays. However the volume of pores in the region of 590–1770 Å (59–177 nm) suggests that macropores are the major pores present in the raw clays. Consequently, in the thermally treated clays, macropores in the range of 630–2018 Å (63–202 nm) as shown in Fig. 4 indicates that the distribution of macropores is higher in the thermally treated clays than in the raw clays. Therefore it can be concluded that high BET surface area, macropores present in the thermally treated clays are desirable properties for its suitability as precursors for supplementary cementitious and geopolymer materials.

3.3 Color and x-ray fluorescence (XRF) analysis of the clays

The colors of the raw clays (Fig. 1) revealed that Ijero-Ekiti clay is white impacted by albite. Ikere-Ekiti is golden yellow but turned brownish red when thermally treated. This brownish red color is due to the presence of high amount of Fe_2O_3 impurity. Isan-Ekiti is creamy white; Abusoro is light pink perhaps due to the presence of montmorillonite as shown by XRD (Fig. 6). Odigbo is greyish white, probably due to the presence of illite in the clay (Fig. 6). The oxide composition (XRF) results of the thermally treated clays (Table 2) showed that the clays consist mainly of SiO_2 (46.4–62.1%) and Al_2O_3 (19.7–41.0%). Alumina and silica are the building blocks for geopolymer formation. Consequently, these clays may be suitable as geopolymer starting materials. The oxide composition indicated that none of the clays is pure kaolinite-containing clays but contained traces of other minerals. The clays contained low content of CaO which is an indication of absence of significant amount of calcite [39]. Ikere-Ekiti and IS have the highest composition of Al_2O_3 which suggested the existence of high amount of kaolinite in the clays [30]. Odigbo and Abusoro have higher amount of silica when compared with IJ, IK and IS, signifying the presence of other clay minerals in addition to kaolinite. Usually, 2:1 clays (e.g. smectite and mica groups) have more silica content and lower alumina than 1:1 clay kaolinite group as reported in previous studies [2, 3, 7, 9, 18]. Odigbo clay on comparison

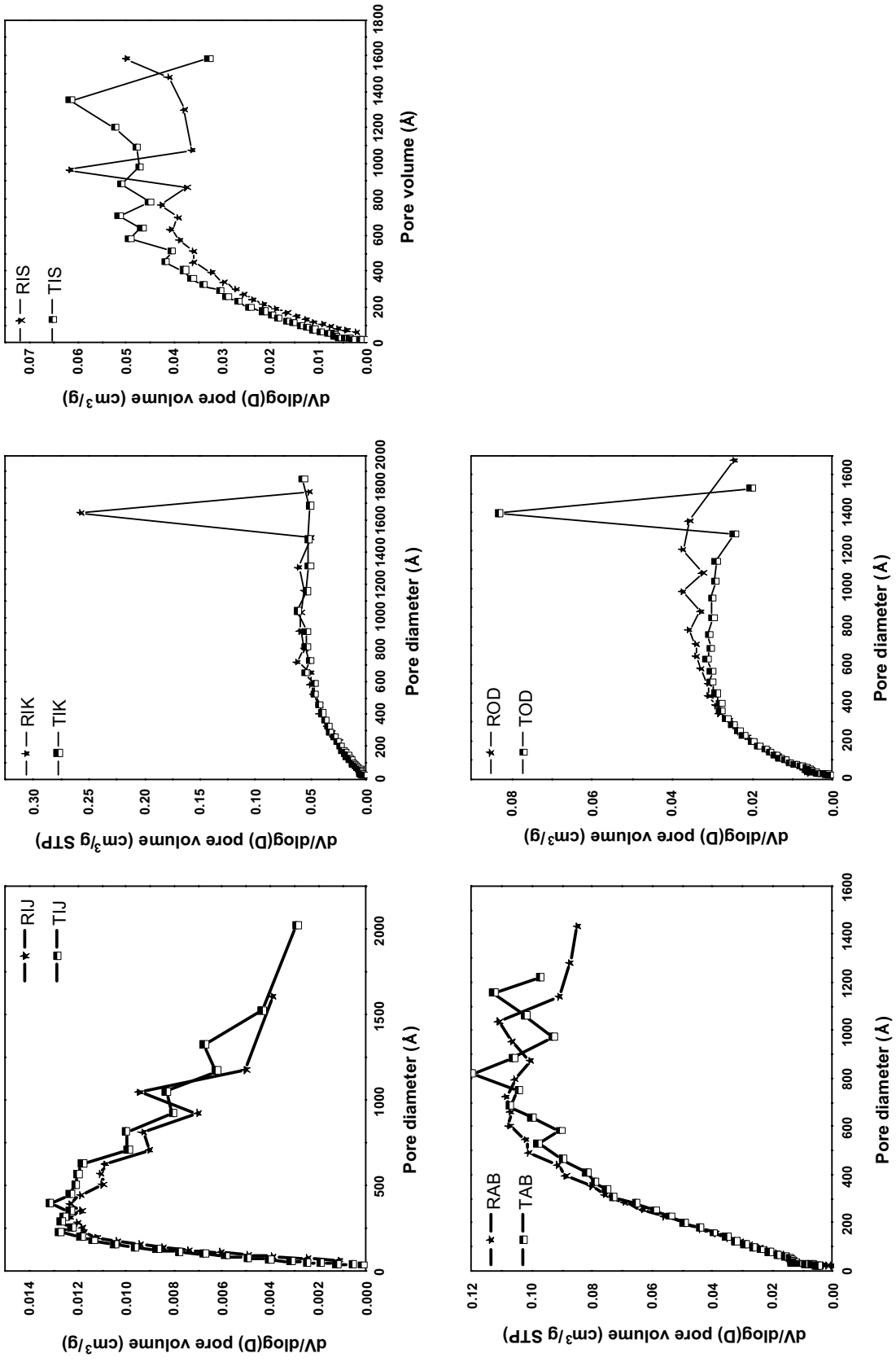

Fig. 4 Barrett–Joyner–Halenda (BJH) pore size distribution of raw and thermally treated Ijero clays (V- pore volume; D-pore diameter)

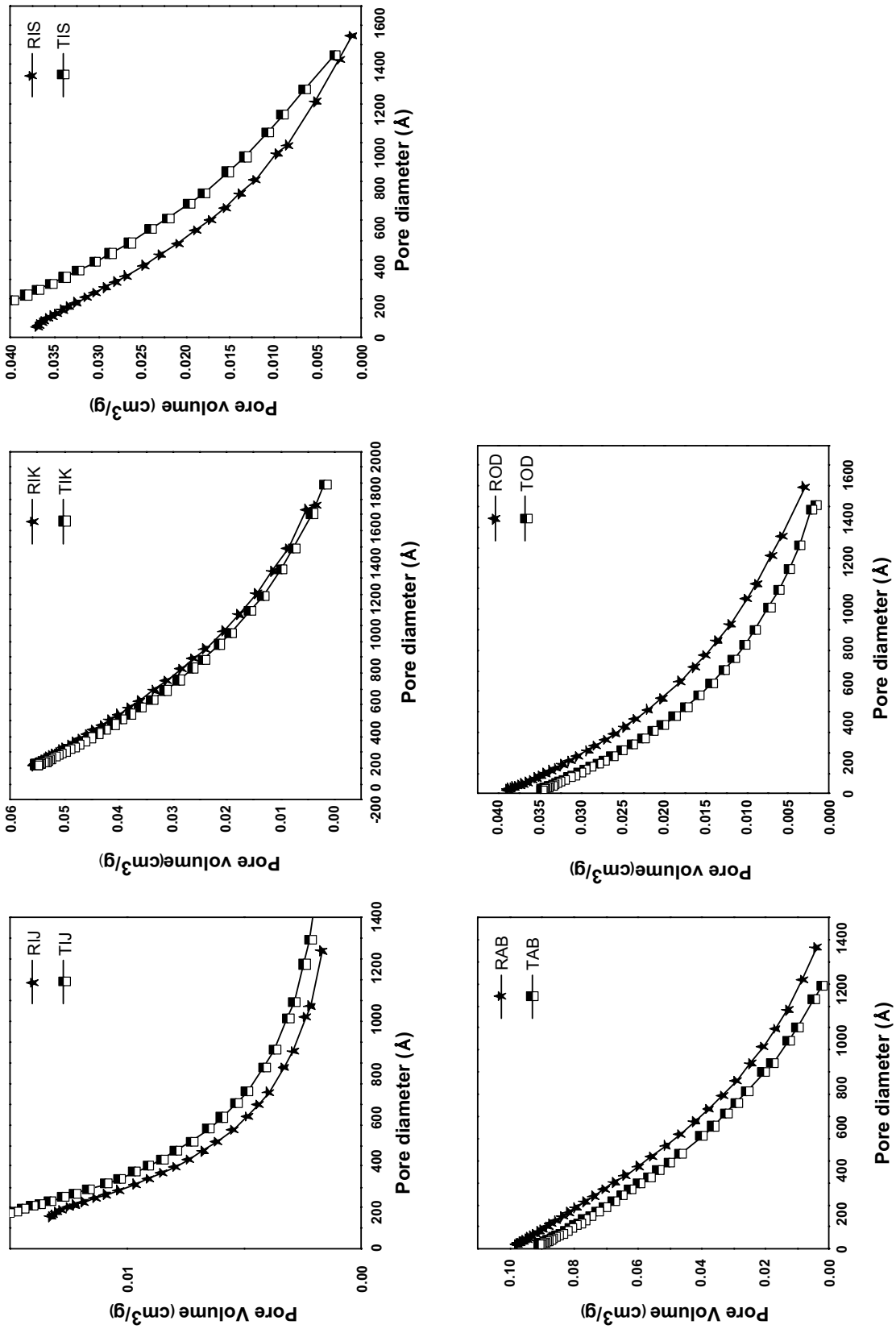

Fig. 5 BJH cumulative pore volume of raw and thermally treated Ijero clay

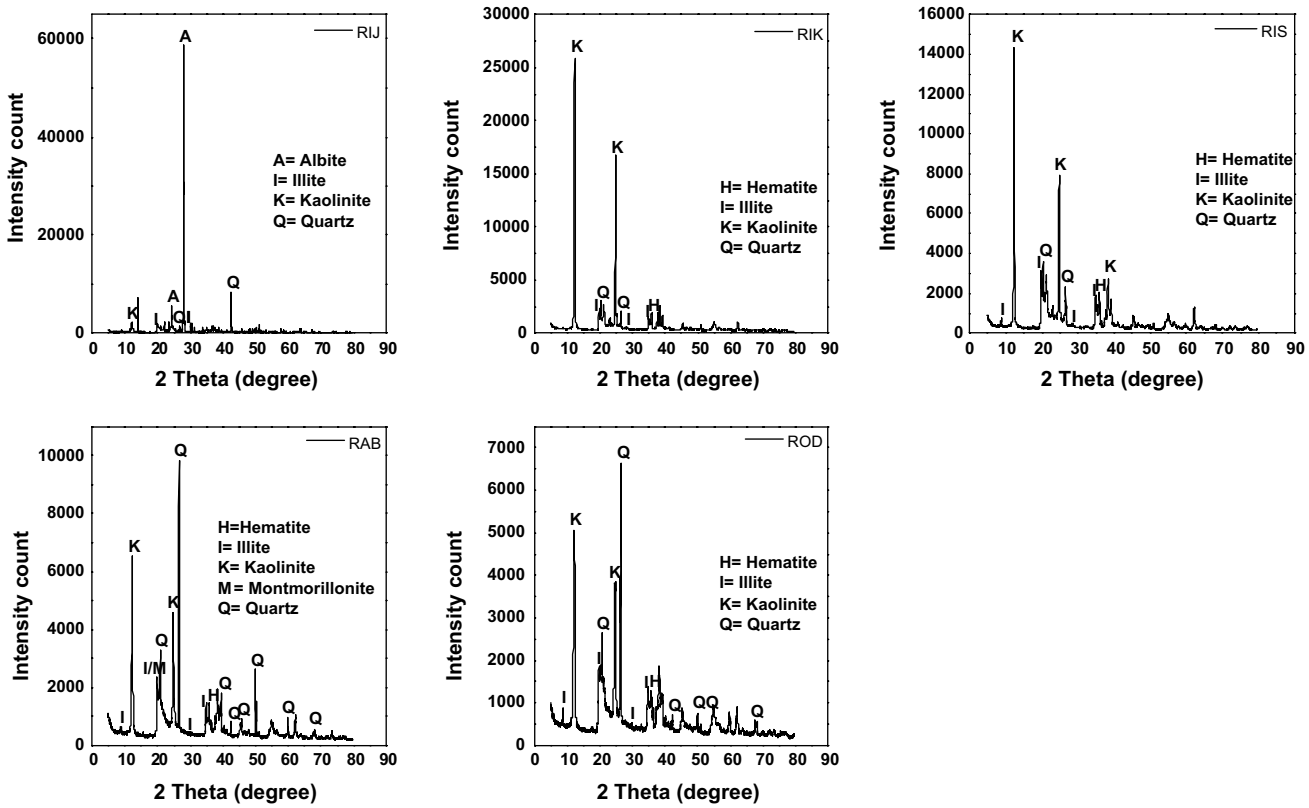

Fig. 6 X-ray diffraction patterns of raw kaolin clays (RIJ = Raw Ijero clay, RIK = Raw Ikere, RIS = Raw Isan clay, RAB = raw Abusoro clay and ROD = Raw Odigbo clay

with others has considerable amount of K_2O, signifying the presence of illite $(K,H_3O)(Al,Mg,Fe)_2(Si,Al)_4O_{10}[(OH)_2,(H_2O)]$. The presence of this mineral was confirmed in the XRD diffractograms of the clays, particularly in OD (Fig. 6). Furthermore, a significant amount of Fe_2O_3 was observed in IK and IS, indicating presence of hematite and was also found in their XRD patterns. The presence of this oxide resulted in the characteristic color displayed by IK and IS (Table 2). These clays may require purification to remove or reduce Fe_2O_3 if they are intended for industrial uses. Ijero-Ekiti has the least percentage composition of Fe_2O_3 (0.10%) compared to Ikere clay (8.51%). This is also revealed in the whitish colour of the clay. Ikere-Ekiti, AB and OD contained anatase; the presence of it was also confirmed by their XRD patterns in thermal state (Fig. 7).

Additionally, the clays except Ijero-Ekiti can be classified as Class N natural pozzolans category of cementitious materials. ASTM C618 (2014) as cited by Lorentz et al. [23] specifies that for natural pozzolans, the sum of SiO_2, Al_2O_3 and Fe_2O_3 must be ≥ 70% by mass and that SO_3 content must not be > 4%. The sum of these oxides in the clays except IJ (66.2%) ranged from 91.9% (IS) to 97.4% (AB), thereby eliminating IJ as pozzolanic material. The SO_3 was only detected in IJ, OD and AB and were less than the stipulated bench mark. Therefore, these clays can be applied as supplementary cementitious materials.

3.4 X-ray diffraction (XRD) analysis

The clay and associated minerals in the raw clays and their transformation in the thermally treated clays were identified using XRD (Figs. 6 and 7). It can be observed that the thermal treatment at the maximum dehydroxylation temperatures caused kaolinite peaks to disappear with appearance of humps at 2θ = 20°–30° while others were retained. In raw IJ, feldspar, in form of albite ($NaAlSi_3O_8$) was predominant with traces of quartz, illite and kaolinite. This Na-feldsper was confirmed by the highest composition of Na_2O in IJ (Table 2). The absence of other forms of feldspar [Anorthite ($CaAl_2Si_2O_8$), orthoclase ($KAlSi_3O_8$)] was confirmed by low amount of CaO and K_2O in IJ (Table 2). Kaolinite peak disappeared in the thermally treated clay, but albite and quartz peaks were retained, indicating that quartz and albite were more resistant to heat treatment than kaolinite. Albite is a sodium feldspar, an aluminosilicate mineral which melts over a wide range of temperatures (1100–1134 °C) as reported in literature [40].

Table 2 X-ray fluorescence analysis of thermally treated clays

Oxides	TIJ	TOD	TIS	TIK	TAB
SiO_2	46.4	61.0	49.2	47.2	62.1
Al_2O_3	19.7	34.4	39.8	41.0	33.6
Fe_2O_3	0.10	1.96	2.90	8.51	1.72
CaO	0.08	0.06	0.04	0.04	0.04
MnO	–	–	0.04	0.01	–
ZnO	0.03	–	0.13	0.15	0.01
NiO	–	0.01	0.09	0.10	0.01
SnO_2	–	–	1.45	1.34	–
P_2O_5	0.07	0.16	0.36	0.38	0.12
SO_3	0.03	0.35	–	–	0.06
Na_2O	2.71	–	–	–	–
K_2O	0.31	0.95	0.33	0.08	0.33
Cr_2O_3	0.04	0.02	–	–	0.03
TiO_2	–	0.86	–	1.86	1.61
V_2O_5	–	0.03	0.02	0.03	–
CuO	–	0.02	0.09	0.08	0.01
SrO	–	0.01	–	0.01	0.01
PbO	–	–	0.05	–	–
Sb_2O_3	–	–	1.26	–	–
SiO_2/Al_2O_3	2.36	1.77	1.24	1.15	1.85
$SiO_2 + Al_2O_3 + Fe_2O_3$ (%)	66.2	97.4	91.9	96.7	97.4
Color	White	Greyish white	Creamy white	Golden yellow	Light pink

– Means not detectable

Its color is commonly white, and its uses commercially include ceramic production when mixed with kaolin and quartz. When it is heated at high temperatures, it fuses and acts as a binder, binding quartz and kaolin. This presents IJ as a potential material for ceramic production since it naturally contains these materials. The XRD peaks of raw IK and IS demonstrated crystalline kaolinite as the dominant clay mineral with traces of illite, quartz and hematite. The presence of hematite in the clay was also confirmed by high amount of Fe_2O_3 (Table 2). It is worthy to note that, unlike IJ, AB and OD, large amount of amorphous materials (metakaolinite) revealed by diffused big humps between 20 and 30° 2θ were observed in the XRD patterns of thermally treated IK and IS (Fig. 7). The amorphous materials suggest the presence of higher proportion of metakaolinite from the thermal transformation of kaolinite in the clays. The high kaolinitic properties of IK and IS are in agreement with the results of TGA/DTA of the clays where the two clays showed higher mass losses at the dehydroxylation temperatures (Fig. 2). The mineralogical composition is also in good agreement with their high silica and alumina content (Table 2). The XRD pattern of raw AB showed the presence of kaolinite, montmorinollite and illite as the clay minerals with traces of quartz and hematite. However, in the thermally treated state, the peaks of kaolinite disappeared and were replaced with amorphous materials due to the transformation of kaolinite to metakaolinite, while those of illite, montmorillonite and quartz are still observable.

The XRD patterns of OD in the raw state indicated the presence of kaolinite, and traces of illite, quartz and hematite. In the thermally treated state, it showed the presence of illite and an amorphous material, which is demonstrated by the hump between 20° and 30° 2θ. It also contained traces of quartz and hematite. The observed amorphous material can be associated with the presence of metakaolinite from the thermal transformation of kaolinite in the clay. The appearance of illite peaks in the XRD patterns of the clays and montmorillonite in AB at the dehydroxylation temperatures suggests that the structures of these clay minerals were still retained at the temperature. Zhou et al. [11] and Wang et al. [31] reported that illite was not fully dehydroxylated until around 850 °C. To improve the amorphous status of these clays, future investigations should include thermal treatment at higher temperatures.

The presence of amorphous materials in the thermally treated IK, IS, AB and OD suggest that when they are used as supplementary cementitious materials, they will show pozzolanic reactivity which can be used in cement and concrete industry. Similarly, when they are used as

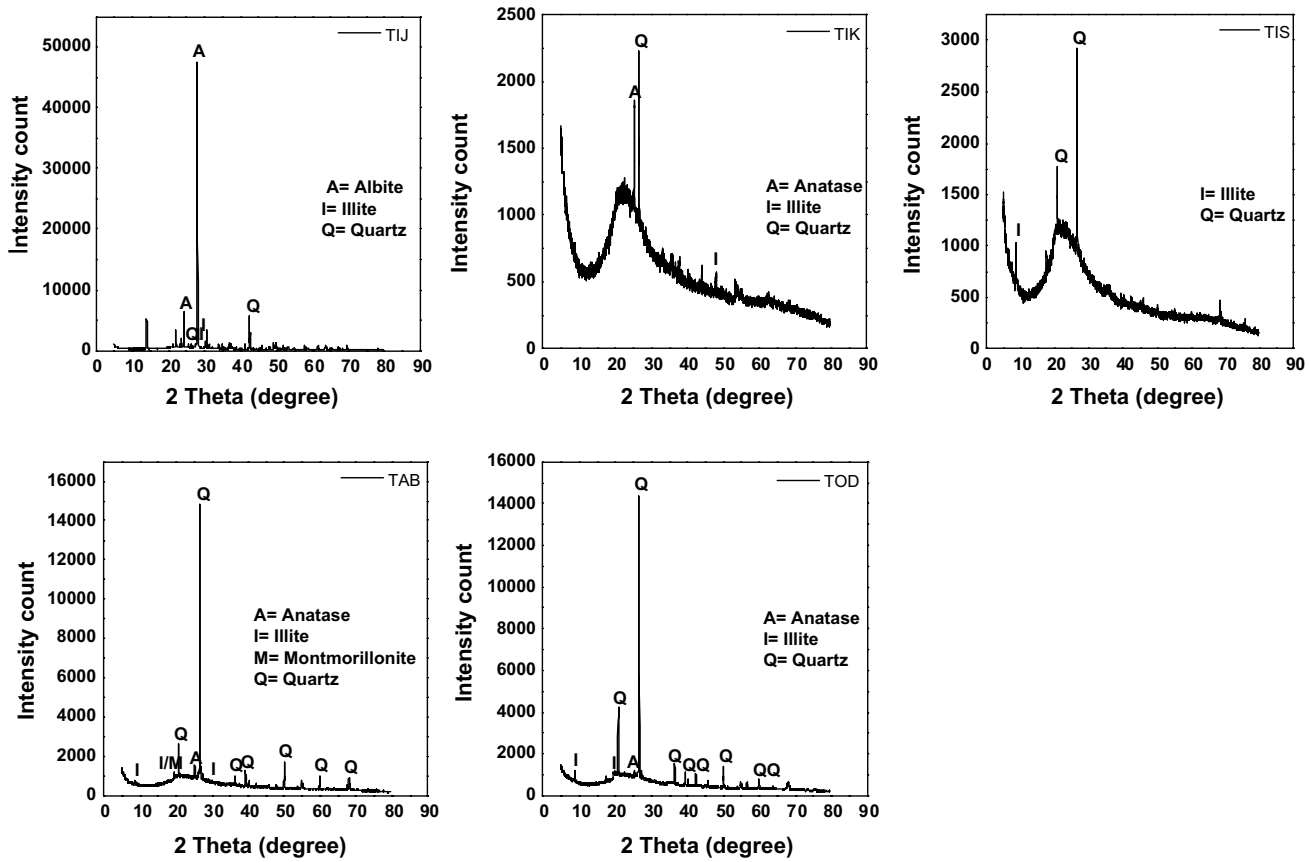

Fig. 7 X-ray diffraction patterns of thermally treated clays

geopolymer materials they will display alkaline reactivity. Quartz and hematite in the clays showed little or no change with thermal treatment.

3.5 Fourier transform Infrared (FTIR) spectroscopy

Infrared spectroscopy was also used to determine the functional groups of minerals that were present in the raw and thermally treated clays. The FTIR spectra of raw and thermally treated clays (Fig. 8) and their major functional groups in the 4000–3000 cm^{-1} and 1300–500 cm^{-1} spectra regions as identified in literature are discussed. For all the raw clays, the OH stretching vibrations typical of the presence of kaolinite occurred at absorption bands 3698-3694 cm^{-1}, and of 2:1 clay minerals (montmorillonite and illite) occurred at absorption bands 3626–3620 cm^{-1} in all the clays [2, 16, 28, 31, 41]. These OH vibrations are due to hydroxyl groups that are attached to aluminium octahedron sheet of the clay minerals. An OH broad stretching vibration at 3437 cm^{-1} and 3434 cm^{-1} was identified in RIK and ROD and this has been attributed to OH vibration of water of hydration on 2:1 clay minerals, particularly illite [31]. Outside this region, bands around 1640 and 1630 cm^{-1} were identified in the spectra of raw IJ, IK, IS, AB and OD clays. These bands were linked with OH bending vibrations of adsorbed water [31, 41]. The bands between 1339 and 1249 cm^{-1} have been assigned to stretching vibrations of Si–O and Al–O bonds in albite ($NaAlSi_3O_8$) confirming the presence of albite in IJ [41].

In the 1300–600 cm^{-1} region, absorption bands associated with Si–O–Si stretching vibrations, which are typical of kaolinite, illite and montmorillonite were observed in the raw IJ, IK, IS, AB, and OD clays at wave numbers 1041, 1032,1033, 1032 and 1031 cm^{-1} respectively [31, 42]. Al(VI)–OH bending vibrations typical of the clay minerals were observed at bands between 914 and 911 cm^{-1} [16, 19, 31] in the clays. The Si–O bending vibrations in the region 600 to 400 cm^{-1} in the clays have been attributed to a couple of stretching-bending vibrations of the cation-oxygen octahedra lying on a similar spectral region [31].

Si–O–Al(VI) bending vibrations due to kaolinite were also observed at bands between 697 and 688 cm^{-1} [16]. Si–O vibrations at around 535 cm^{-1} and between 471 and 469 cm^{-1} were observed and associated with the presence of quartz [16, 19]. These observations confirm the presence of kaolinite in all the clays. The absorption

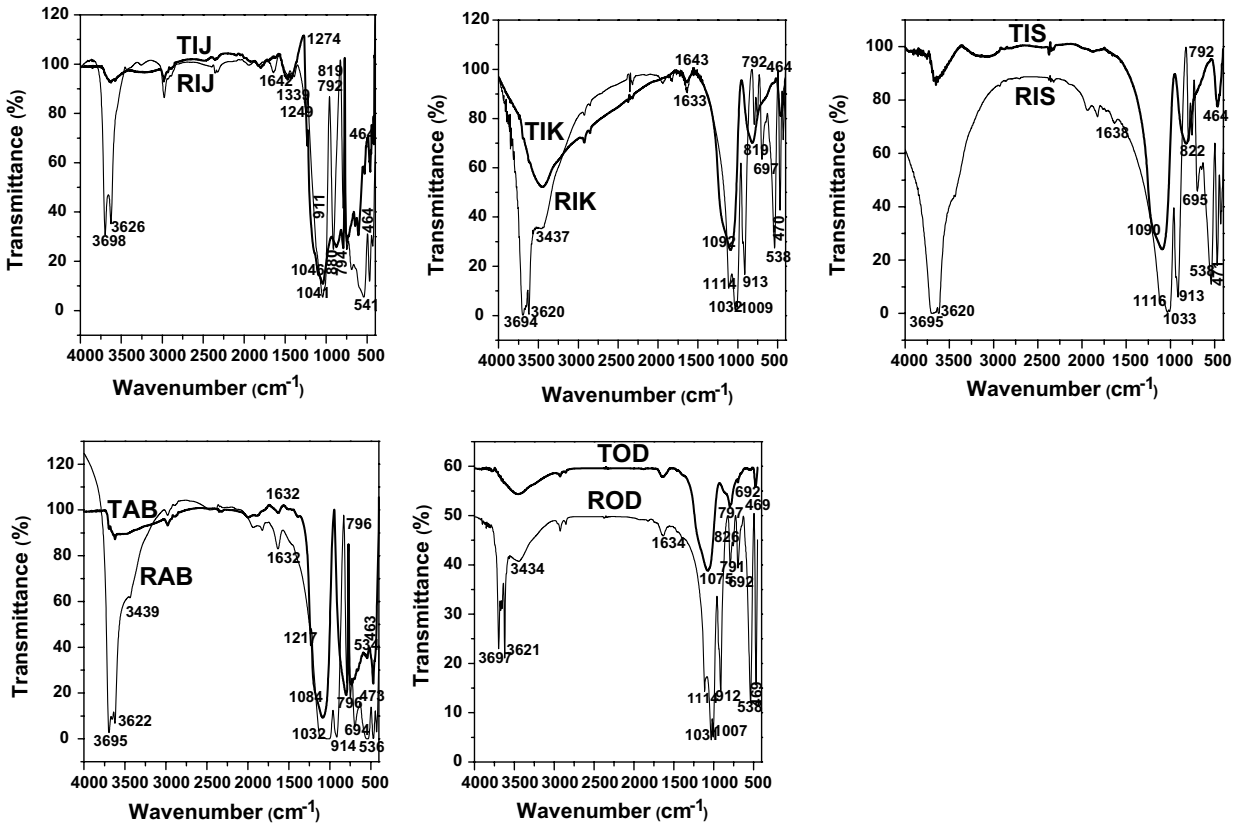

Fig. 8 FTIR spectra of raw and thermally treated clays

bands at 792, 697, 695, 796 and 692 cm^{-1} were observed for RIJ, RIK, RIS, RAB and ROD, respectively and these have been associated with the Si–O stretching frequencies of quartz [11, 32]. These bands are typical of quartz in kaolinite, montmorillonite and illite.

Remarkable changes were observed in the FTIR spectra of the thermally treated clays compared to the raw clays. The broad bands of the OH groups at 4000–3000 cm^{-1} spectra region in the raw clays that indicated the presence of crystalline kaolinite disappeared at the dehydroxylation temperature of each clay. This was replaced by low intensity broad bands typical of 2:1 clay minerals [12]. These authors documented that the absorption band of montmorinollite decreased with increasing temperature above 600 °C and could not be detected at temperature up to 925 °C, confirming that at the dehydroxylation temperature of kaolinite, the structure of montmorillonite is less severely disturbed. The size of this band was peculiar for each of the five clays. It was observed that it was biggest for IK and least for IJ. This was also reflected in the amount of weight loss at the third endothermic reaction of these clays. Mass losses of 0.03, 0.07, 1.11, 1.22 and 2.12% were observed at the third endothermic peaks for IJ, OD, AB, IS and IK. The XRD patterns confirmed the presence of illite in all the clays together with montmorillonite in AB only.

Three prominent absorption bands between 1116 and 1031 cm^{-1} were replaced with broad bands in the thermally treated clays at wave number between 1092 and 1046 cm^{-1} [16, 19]. Al (VI)–OH bending vibrations at bands between 914 and 911 cm^{-1} in the raw clays disappeared and new bands which indicating that tetrahedral coordination Al(IV)–O stretching vibrations appeared at 797, 822, 819 and 796 cm^{-1} for TOD, TIS, TIK and TAB respectively. The Si–O–Al bending vibrations bands between 541 and 535 cm^{-1}, were replaced by Si–O in-plane bending vibration at 463 and 469 cm^{-1} in all the thermally treated clays [16, 19].

The FTIR results confirmed the presence of kaolinite in the raw clays and transformation of kaolinite to metakaolinite in the thermally treated clays. The XRD patterns were consistent with FTIR spectra of both raw and thermally treated clays.

4 Conclusion

Thermal, surface area, oxide and mineralogical composition, and structural properties of raw and thermally treated five local kaolin clays from South-West Nigeria were characterized. The BET surface area values increased from the raw clays to the thermally treated clays. Combining the results of TGA/DTA, XRF, XRD and FTIR, Ijero-Ekiti clay was identified as feldspar (albite)-quartz containing clay with traces of kaolinite and illite, Ikere-Ekiti and Isan-Ekiti clays were classified as kaolinite-dominated clays with traces of hematite, illite, quartz and anatase. Abusoro clay contained kaolinite primarily with small amounts of illite, montmorillonite, hematite and quartz and Odigbo clay contained kaolinite and trace amounts of illite, hematite and quartz. There were good agreements among TGA/DTA, XRD and FTIR results which confirmed the transformation of kaolinite in the raw clays to metakaolinite in the thermally treated clays. Based on the properties displayed, it can be concluded that when clays from Ikere-Ekiti, Isan-Ekiti, Abusoro and Odigbo deposits are thermally treated, they have potentials to form useful supplementary cementitious and geopolymer materials to make binders in building and construction while clay from Ijero-Ekiti deposit can serve as ceramic material. Further investigations are required to determine the pozzolanic activity, alkaline silicate reactivity and ceramic formation potentials of the thermally treated clays.

Acknowledgements The authors thank The World Academy of Sciences (TWAS) for financial support for Funmilayo I. Adeniyi under Sandwich Postgraduate Fellowships to Young Scientists from Developing Countries. The Director, CSIR- Structural Engineering Research Center, Chennai, India, is gratefully acknowledged for making available the research facilities for this study.

Author contributions Author A received research grant from The Council of Scientific and Industrial Research (CSIR) and The World Academy of Sciences (TWAS) Sandwich Postgraduate Fellowship Award. Author B is a member of the following Royal Society of Chemistry interest groups; Analytical Division, Applied Materials Chemistry Group, Environmental Chemistry Group. Conceptualization: [Mary B. Ogundiran (PhD), Funmilayo I. Adeniyi (MSc)], Methodology: [Mary B. Ogundiran, Funmilayo I. Adeniyi, T. Hemalatha (PhD)], Formal analysis and investigation: [Funmilayo I. Adeniyi], Writing- original draft preparation: [Funmilayo I. Adeniyi], Writing- review and editing: [Mary B. Ogundiran, Funmilayo I. Adeniyi, T. Hemalatha, Bhajantri. H. Bharatkumar (PhD)], Funding acquisition [2016 CSIR-TWAS Sandwich Postgraduate Fellowship; CSIR-Structural Engineering Research Center, Chennai, India], Resources: [T.Hemalatha, Bhajantri. H. Bharatkumar], Supervision: [Mary B. Ogundiran, T. Hemalatha, Bhajantri. H. Bharatkumar].

Funding This study was funded by The Council of Scientific and Industrial Research (CSIR) and The World Academy of Sciences (TWAS) Sandwich Postgraduate Fellowship Award (FR number: 3240293582).

Data availability The datasets generated during the current study are available in the Mendeley Repository, https://dx.doi.org/10.17632/hp3pnkk225.1.

Compliance with ethical standards

Conflict of interest The authors declare that they have no conflict of interest.

References

1. Yaya A, Tiburu EK, Vickers ME, Efavi JK, Onwona-Agyeman B, Knowles KM (2017) Characterisation and identification of local kaolin clay from Ghana: a potential material for electroporcelain insulator fabrication. Appl Clay Sci 150:125–130. https://doi.org/10.1016/j.clay.2017.09.015
2. Favero JS, Parisotto-Peterle J, Weiss-Angeli V, Brandalise RN, Gomes LB, Bergmann CP, Santos V (2016) Physical and chemical characterization and method for the decontamination of clays for application in cosmetics. Appl Clay Sci 124–125:252–259. https://doi.org/10.1016/j.clay.2016.02.022
3. Hedfi I, Hamdi N, Srasra E, Rodriguez MA (2014) The preparation of micro-porous membrane from a Tunisian kaolin. Appl Clay Sci 101:574–578. https://doi.org/10.1016/j.clay.2014.09.021
4. Qoniah I, Prasetyoko D, Bahruji H, Triwahyono S, Jalil AA, Suprapto H, Purbaningtias TE (2015) Direct synthesis of mesoporous aluminosilicates from Indonesian kaolin clay without calcination. Appl Clay Sci 118:290–294. https://doi.org/10.1016/j.clay.2015.10.007
5. Pan F, Lu X, Wang T, Wang Y, Zhang Z, Yan Y, Yang S (2013) Synthesis of large mesoporous γ-Al_2O_3 from coal-series kaolin at room temperature. Mater Lett 91:136–138. https://doi.org/10.1016/j.matlet.2012.09.052
6. Faqir NM, Elkatatny S, Mahmoud M, Shawabkeh R (2017) Fabrication of kaolin-based cement plug for CO_2 storage wells. Appl Clay Sci 141:81–87. https://doi.org/10.1016/j.clay.2017.02.011
7. Schulze SE, Rickert J (2019) Suitability of natural calcined clays as supplementary cementitious material. Cem Concr Compos 95:92–97. https://doi.org/10.1016/j.cemconcomp.2018.07.006
8. El-Diadamony H, Amer AA, Sokkary TM, El-Hoseny S (2018) Hydration and characteristics of metakaolin pozzolanic cement pastes. HBRC J 14:150–158. https://doi.org/10.1016/j.hbrcj.2015.05.005
9. Danner T, Norden G, Justnes H (2018) Characterisation of calcined raw clays suitable as supplementary cementitious materials. Appl Clay Sci 162:391–402. https://doi.org/10.1016/j.clay.2018.06.030
10. Shah V, Bishnoi S (2018) Carbonation resistance of cements containing supplementary cementitious materials and its relation to various parameters of concrete. Const Build Mater 178:219–232. https://doi.org/10.1016/j.conbuildmat.2018.05.162
11. Zhou D, Wang R, Tyrer M, Wong H, Cheeseman C (2017) Sustainable infrastructure development through use of calcined excavated waste clay as a supplementary cementitious material. J Clean Prod 168:1180–1192. https://doi.org/10.1016/j.jclepro.2017.09.098
12. Alujas A, Fernandez R, Quintana R, Scrivener KL, Martirena F (2015) Pozzolanic reactivity of low grade kaolinitic clays: influence of calcination temperature and impact of calcination products on OPC hydration. Appl Clay Sci 108:94–101. https://doi.org/10.1016/j.clay.2015.01.028

13. Shvarzman A, Kovler K, Grader GS, Shter GE (2003) The effect of dehydroxylation/amorphization degree on pozzolanic activity of kaolinite. Cem Concr Res 33:405–416
14. Liu Y, Lei S, Lin M, Li Y, Yea Z, Fan Y (2017) Assessment of pozzolanic activity of calcined coal-series kaolin. Appl Clay Sci 143:159–167. https://doi.org/10.1016/j.clay.2017.03.038
15. Kakali G, Perraki T, Tsivilis S, Badogiannis E (2001) Thermal treatment of kaolin: the effect of mineralogy on the pozzolanic activity. Appl Clay Sci 20:73–80
16. Ogundiran MB, Kumar S (2015) Synthesis and characterisation of geopolymer from Nigerian clay. Appl Clay Sci 108:173–181. https://doi.org/10.1016/j.clay.2015.02.022
17. Kuenzel C, Li L, Vandeperre L, Boccaccini AR, Cheeseman CR (2014) Influence of sand on the mechanical properties of metakaolin geopolymers. Constr Build Mater 66:442–446. https://doi.org/10.1016/j.conbuildmat.2014.05.058
18. Seiffarth T, Hohmann M, Posern K, Kaps C (2013) Effect of thermal pre-treatment conditions of common clays on the performance of clay-based geopolymeric binders. Appl Clay Sci 73:35–41. https://doi.org/10.1016/j.clay.2012.09.010
19. Davidovits J (2011) Geopolymer: chemistry and applications, 3rd edn. Institut Geopolymere, France
20. Provis JL, Yong SL, Duxson P (2009) (2009) Nanostructure/microstructure of metakaolin geopolymers. Geopolymers. In: Provis JL, van Deventer JSJ (eds) Structure, processing, properties and industrial applications. Woodhead Publishing Limited, Oxford, pp 72–88
21. Heller-Kallai L (2013) Thermally modified clay minerals. In: Bergaya F, Lagaly G (eds) Handbook of clay science. Developments in Clay Science, vol 5A. Elsevier Ltd, pp 411–433
22. Mendelovici E (1997) Comparative study of the effects of thermal and mechanical treatments on the structures of clay minerals. J Therm Anal 49:1385–1397
23. Lorentz B, Shanahan N, Stetsko YP, Zayed A (2018) Characterization of Florida kaolin clays using multiple-technique approach. Appl Clay Sci 161:326–333. https://doi.org/10.1016/j.clay.2018.05.001
24. Ekpunobi UE, Agboa SU, Ajiwe VIE (2019) Evaluation of the mixtures of clay, diatomite, and sawdust for production of ceramic pot filters for water treatment interventions using locally sourced materials. J Environ Chem Eng 7:102791
25. Obada DO, Dodoo-Arhin D, Dauda M, Anafi FO, Ahmed AS, Ajayi OA (2017) The impact of kaolin dehydroxylation on the porosity and mechanical integrity of kaolin based ceramics using different pore formers. Results Phys 7:2718–2727. https://doi.org/10.1016/j.rinp.2017.07.048
26. Bergaya F, Lagaly G (2013) General introduction: clays, clay minerals, and clay science. In: Bergaya F, Lagaly G (eds) Handbook of clay science. Developments in Clay Science, vol 5A. Elsevier Ltd, 2013, pp 1–19
27. Brigatti MF, Galan E, Theng BKG (2013) Structure and mineralogy of clay minerals. In: Bergaya F, Lagaly G (eds) Handbook of clay science. Developments in Clay Science, vol 5A. Elsevier Ltd, pp 21–81
28. Ndzana GM, Huang L, Zhang Z, Zhu J, Liu F, Bhattacharyya R (2019) The transformation of clay minerals in the particle size fractions of two soils from different latitude in China. CATENA 175:317–328. https://doi.org/10.1016/j.catena.2018.12.026
29. Cheng K, Heidari Z (2017) Combined interpretation of NMR and TGA measurements to quantify the impact of relative humidity on hydration of clay minerals. Appl Clay Sci 143:362–371. https://doi.org/10.1016/j.clay.2017.04.006
30. Almenares RS, Vizcaino LM, Damas S, Mathieu A, Alujas A, Martirena A (2017) Industrial calcination of kaolinitic clays to make reactive pozzolans. Case Stud Constr Mater 6(225):232. https://doi.org/10.1016/j.cscm.2017.03.005
31. Wang G, Wang H, Zhang N (2017) In situ high temperature X-ray diffraction study of illite. Appl Clay Sci 146:254–263. https://doi.org/10.1016/j.clay.2017.06.006
32. Serra MF, Conconi MS, Suarez G, Agietti EF, Rendtorff NM (2013) Firing transformations of an argentinean calcareous commercial clay. Ceramica 59:254–261
33. Ibisi M (1992) A feldspar sample from Nigeria. Bol Soc Esp Ceram Vidr 31(2):127–130
34. Grim RE, Kulbicki (1961) Montmorillonite: high temperature reactions and classifications. Am Miner 46
35. Kenne Diffo BB, Elimbi A, Cyr M, Dika Manga J, Tchakoute Kouamo H (2015) Effect of the rate of calcination of kaolin on the properties of metakaolin-based geopolymers. J Asian Ceram Soc 3:130–138
36. Acevedo NI, Rocha MCG, Bertolino LC (2017) Mineralogical characterization of natural clays from Brazillian Southeast region for industrial applications. Ceramica 63:253–262
37. Sing KSW, Everett DH, Haul RAW, Moscou L, Pierotti RA, Rouquerol J, Siemieniewska T (1985) Reporting physisorption data for gas/solid systems with special reference to the determination of surface area and porosity. Pure Appl Chem 57(4):603–619
38. Anovitz LM, Cole DR (2015) Characterization and analysis of porosity and pore structures. Rev Min Geochem 80:61–164
39. Ravisankar R, Naseerutheen A, Rajalakshmi A, Annamalai GR, Chandrasekaran A (2014) Application of thermogravimetry-differential thermal analysis (TG-DTA) technique to study the ancient potteries from Vellore dist, Tamilnadu, India. Mol Biomol Spectrosc 129:201–208. https://doi.org/10.1016/j.saa.2014.02.095
40. Johnson LA, McCauley RA (2005) The thermal behavior of albite as observed by DTA. Thermochim Acta 437:134–139
41. Hahn A, Vogel H, Ando S, Garzanti E, Kuhn G, Lantzsch H, Schuurman J, Vogt C, Zabel M (2018) Using Fourier transform infrared spectroscopy to determine mineral phases in sediments. Sediment Geol 375:27–35. https://doi.org/10.1016/j.sedgeo.2018.03.010
42. D'Elia A, Pinto D, Eramo G, Giannossa LC, Ventruti G, Laviano R (2018) Effects of processing on the mineralogy and solubility of carbonate-rich clays for alkaline activation purpose: mechanical, thermal activation in red/ox atmosphere and their combination. Appl Clay Sci 152:9–21. https://doi.org/10.1016/j.clay.2017.11.036